Less-Concentrated HPAM Solutions as a Polymer Retention Reduction Method in CEOR

Lizcano Nino J.C*; Ferreira Vitor Hugo de Sousa; Moreno Rosangela B. Z. L

ORCID: https://orcid.org/0000-0001-5216-4638

Mechanical Engineering School, University of Campinas (UNICAMP), Campinas - SP, Brasil.

Email: juan.lizcano.25@gmail.com

Abstract

Polymer Flooding has become one of the most implemented EOR techniques, due to three factors: First, Polymer flooding has expanded the range of the screening criteria parameters. Second, this EOR method is more effective than water injection, while handling water management issues in high water-cut reservoirs. Nevertheless, polymer retention can turn a viable technical project into an uneconomical one. Polymer loss due to retention is an inevitable phenomenon, which happens during injection processes. The development of experimental analysis aiming to minimize or reduce polymer loss from the displacing fluid bank is beneficial to broaden the application of this CEOR method. This experimental work evaluated the injection schemes aiming to reduce polymer retention in porous media. The approach consisted of injecting less-concentrated polymer banks followed for the main polymer bank designed for mobility control. An experimental methodology to quantify polymer retention due to each injected polymer bank, cumulative polymer retention, resistance factor, residual resistance factor and inaccessible pore volume (IPV) was developed. The measurement process was based on the injection of 20 PV polymer banks at a constant flow rate of 1ml/min at 25°C, separated by 30 PV brine banks. Two HPAM with molecular weights of 6-8 million and 20 million Daltons using 350mD and 5000 mD sandstone cores were tested, respectively. The HPAM solutions considering a Colombian field (0.7% NaCl) and seawater (3.5% TDS) salinities were prepared. All rock samples were previously submitted to the injection of 50 PV for preventing fines migration. Two injection schemes with variable polymer concentrations were performed: The first one in which the polymer concentration increased in each successive bank, and the second one in which the concentration decreased. HPAM concentration solutions from 50 ppm to 2000 ppm were sequentially used in both injection schemes. By comparing the results of these two schemes, the effect of the injection of the less-concentrated polymer solutions was evaluated. For the increasing concentration experiments, cumulative retention values of 175.7 µg/g and 58.9 µg/g were calculated for the low-molecular weight polymer and the high-molecular weight polymer, respectively. While comparing with decreasing concentration experiments, for the high-molecular weight HPAM a 19% of retention reduction was evidenced, but no retention reduction was observed for the low-molecular weight one. The results indicate that different retention mechanisms are strongly dependents on the absolute permeability of the samples. Additionally, IPV values of 0.5 PV and 0.25 PV were calculated using low and high permeability samples, respectively. There was no linear relation between the absolute permeability reduction and the polymer concentration of the first bank injected into the sample. The novelty of this work is to use sacrificial banks of less-concentrated HPAM solutions as a reducing retention agent for the polymer bank designed for mobility control.

Keywords: Polymer Flooding; Chemical Flooding; Polymer Retention; Enhanced Oil Recovery; Sandstone.

Soluciones HPAM de baja concentración como método de reducción de la retención de polímeros en CEOR

Resumen

La maduración de la tecnología de inyección de polímeros ha brindado en las últimas décadas rangos de aplicación mayores que otros métodos EOR, principalmente debido al mejoramiento del factor de recobro de petróleo y el gerenciamiento del agua en yacimientos off-shore o en yacimientos heterogéneos. No obstante, la retención de polímeros puede convertir un proyecto viable tecnicamente, en uno no económico. La pérdida de polímero debido a la retención es un fenómeno inevitable, que ocurre en todo proceso EOR con polímeros. El desarrollo de métodos para reducir la pérdida de polímero debido a este fenómeno es benéfico para ampliar la aplicación de este método CEOR. Este trabajo experimental evaluó esquemas de inyección para reducir la retención de polímeros en medios porosos en dos diferentes escenarios de ambiente petrofísico. El enfoque consistió en inyectar

Cita: Lizcano Niño, J. C., De Sousa, V. H. & Moreno, R. B. Z. L (2020). Less-Concentrated HPAM Solutions as a Polymer Retention Reduction Method in CEOR. *Revista Fuentes: El reventón energético, 18*(1), 75-92.

DOI: http://dx.doi.org/10.18273/revfue.v17n1-2020008

baches de polímeros menos concentrados seguidos del banco de polímero principal diseñado para el control de la movilidad. Se desarrolló una metodología experimental para cuantificar la retención de polímero debido a cada banco de polímero inyectado, la retención acumulada de polímeros, el factor de resistencia, el factor de resistencia residual y el volumen de poroso inaccesible (IPV). El proceso de medición se basó en la inyección de 20 bancos de polímeros de PV a un caudal constante de 1 ml / min a 25 ° C, separados por 30 bancos de salmuera de PV. Se probaron dos HPAM con pesos moleculares de 6-8 millones y 20 millones de Daltons, y como medio poroso núcleos de arenisca de 350 mD y 5000 mD, respectivamente. Se prepararon las soluciones HPAM considerando una salinidad de campo colombiano (0.7% de NaCl) y agua de mar (3.5% TDS). Todas las muestras de roca fueron previamente sometidas bajo la inyección de 50 PV para evitar la migración de finos. Se realizaron dos esquemas de inyección con concentraciones variables de polímero: uno en el que la concentración del polímero aumentó en cada banco sucesivo, y otro en el que la concentración disminuyó. Las soluciones de concentración de HPAM de 50 ppm a 2000 ppm se utilizaron secuencialmente en ambos esquemas de inyección. Al comparar los resultados de estos dos esquemas, se evaluó el efecto de la inyección de las soluciones de polímeros menos concentradas. Para los experimentos de concentración creciente, se calcularon valores de retención acumulados de 175.7 µg/g usando polímero de bajo peso molecular y 58.9 µg/g con el polímero de alto peso molecular. Al comparar con experimentos de concentración decreciente, para el HPAM de alto peso molecular se evidenció un 19% de reducción de la retención, debido a que unicamente se evidenció el mecanismo de adsorción quimica de polimero en el medio poroso, sin embargo no se identificó una reducción de la retención para el de bajo peso molecular. Los resultados indican que los diferentes mecanismos de retención dependen en gran medida de la permeabilidad absoluta de las muestras. Además, los valores de IPV de 0.5 PV y 0.25 PV se calcularon utilizando muestras de permeabilidad alta y baja, respectivamente. No hubo una relación lineal entre la reducción de la permeabilidad absoluta y la concentración de polímero del primer banco inyectado en la muestra. La novedad de este trabajo es utilizar bancos de sacrificios de soluciones HPAM menos concentradas como agente de retención reductor para el banco de polímeros diseñado para el control de la movilidad.

Palabras clave: Inyección de polimeros; CEOR; Retención de polímeros; EOR; Recobro Mejorado; Arenisca.

Introduction

Globally, the total demand for primary energy will increase from 273.9 mboe/d in 2014 to 382.1 mboe/d in 2040, representing a rise of 40%. Currently, fossil fuels (oil, gas, and coal) stands for 81% of global energy consumption (OPEC, 2017). In 2040, fossil fuels will maintain their importance in global energy consumption, although with a lower contribution of 77% in the total energy demand (OPEC, 2017). In recent years, world reserves did not record a significant increase to meet future energy needs, with a value of 1700 billion barrels at the end of 2014, sufficient to meet 52.5 years of global production (BP, 2015). Most of the current world oil production comes from mature fields, evidencing the decay of new significant discoveries in the last decades to replace and increase the existing reserves. To supply that energy demand in the coming years, it is necessary to produce the recoverable oil by the implementation of IOR and EOR methods in a scenario of technical and economic feasibility.

The enhanced oil recovery by polymer flooding appears to remedy problems presented in water injection, increasing the water viscosity and reducing the permeability to the aqueous phase (Hatzignatiou *et al.,* 2013; Aya *et al.*, 2018). Polymer solutions are designed to develop a favorable mobility ratio between the ºinjected polymer solution and the oil displaced ahead of the polymer. Therefore, a stable volumetric sweep takes place improving macroscopic sweep efficiency (Green and Willhite, 1998; Sun *et al.*, 2018). However, sometimes this polymer injection is not economically feasible due to excessive retention of polymer in the reservoir (Broseta *et al.,* 1995). During injection, part of the polymer is retained in the porous media due to mechanical entrapment in pores smaller than the size of the polymer molecule, adsorption on the rock surface and hydrodynamic retention induced by the interstitial velocity variation (Gogarty, 1967; Dawson and Lantz, 1972; Szabo, 1975; Huh *et al.,* 1990; Green and Willhite, 1998; Zhang and Seright, 2014; Molano, Navarro and Diaz, 2014). The significance of mechanical entrapment depends on the pore size distribution. It is a more probable mechanism for polymer retention in low-permeability formation (Szabo, 1975; Dominguez and Willhite, 1977; Sorbie, 1991; Sheng, 2010). The retention causes a viscosity reduction of the injected polymer solution and the delay in its propagation (Pinto, Herrera and Angarita, 2018). Thus, this phenomenon understanding is essential for establishing the appropriate retention behavior, which affects directly the economic and technical feasibility of the project (Sorbie, 1991).

Polymer type (Szabo, 1979; Sorbie, 1991), the salinity of the solvent (Martin *et al.,* 1983, Sheng, 2010; Hernandez, Niño and Moreno, 2018; Toro *et al.*, 2018), rock surface type (Szabo, 1979; Sheng, 2010), the molecular weight of the polymer (Gramain and Myard, 1981; Sheng, 2010), hydrolysis degree (Chen and Chen, 2002; Sheng, 2010),

sample permeability (Vela *et al.,* 1976) and temperature (Chen and Chen, 2002; Araujo and Araujo, 2018) are some parameters that affect polymer retention that have been widely discussed. However, the effect of polymer concentration on polymer retention seems controversial (Zhang and Seright, 2014). Some authors suggest Langmuir isotherm to describe polymer retention as a function of its concentration. Nevertheless, Dawson and Lantz (1972), Szabo (1975), Cardozo *et al.,* (2007) performed tests using a static process to achieve this empirical correlation. A dynamic measurement is more realistic to simulate polymer injection process in the reservoir. Zheng *et al.* (2000) implemented an injection scheme varying the polymer concentration in medium permeability sandstones, where polymer solutions with concentrations from 250 ppm through 1500 ppm were injected. Their results showed retention values increasing from 40 µg/g at 250 ppm to 58 µg/g at 1500 ppm. Zhang and Seright (2014) attempted to explain polymer retention and its concentration dependence at dynamic conditions. They used a possible method to minimize polymer retention in porous media. It is suggested by reducing the polymer retention caused by subsequent polymer banks injected. The less-concentrated banks were initially injected, and they were in charge of inducing initial polymer retention in porous media. Then, the subsequent polymer molecules injected will not have rock zones where could occur the retention by chemical adsorption. Final retention values of 16 µg/g due to HPAM 3230S injection from 20 ppm through 1000 ppm and 56 µg/g at 1000 ppm were calculated, which was 3.5 times higher than that obtained in the first core-flooding test.

The inaccessible pore volume is one of the factors that most affect the polymer retention and it is defined as the pore volume fraction that the polymer molecules were not able to access, but accessible to the small solvent and salt molecules during the polymer flooding. (Dawson and Lantz, 1972; Szabo, 1975; Gupta, 1978; Lotsch *et al.,* 1985; Huh *et al.,* 1990; Hughes *et al.,* 1990; Mezzomo *et al.,* 2002; Pancharoen *et al.,* 2010; Ferreira and Moreno; 2017). IPV causes an acceleration on polymer propagation, meanwhile, polymer retention delays this propagation (Zhang and Seright, 2014). Lotsch *et al.,* (1985) proved that it is possible to determinate the IPV by using inorganic salts as tracers, also established that IPV is not affected regarding polymer concentration and the presence of oil in the sample.

This work aims to evaluate the effect of less-concentrated HPAM solutions as a polymer retention reduction method in sandstones. Four displacement tests were performed to quantify polymer retention, inaccessible pore volume (IPV), resistance factor, and absolute permeability reduction due to each polymer bank. The experimental design was adapted to simulate two scenarios, the first one was a low permeability on-shore reservoir with a Total Dissolved Solids content from a Colombian field, and the second one was a high permeability off-shore reservoir using a high molecular weight polymer prepared with seawater Total Dissolved content.

Materials and Methods

Polymers. The SNF Flopaam 3230S and 3630S partially hydrolyzed polyacrylamides (HPAM) were used in tests **(Table 1)**. Polymer solutions were prepared according to the standard API RP 63 (API, 1990). A 5000 ppm stock solution using the magnetic stirrer vortex method was prepared, and from it, HPAM solutions of 50, 100, 500, 1000, and 2000 ppm were diluted. The stock polymer solution was stirred continuously at nearly 100-200 rpm during at least 24-36 hours at room temperature to ensure full hydration of the polymer powder.

Table 1. HPAM polymer used in the experiments.

HPAM Polymer	Molecular Weight	Hydrolysis Degree (%)
3230S	6-8 million Daltons	30
3630S	20 million Daltons	30

Source: SNF Floerger, 2012; Hatzignatiou *et al.,* 2013; Chen *et al.,* 2016.

Brines

Two synthetics brines to represent different scenarios of salt composition were prepared. These brines were used as the base fluid for the preparation of the polymer solutions (Table 2). Deionized and degassed water was used as a solvent in all the fluids according to ASTM D1193-6 (ASTM, 2011). The brine-SF simulated the preparation water composition used in the Colombian San Francisco field (Cortes *et al.,* 2016). This brine had an equivalent salinity of 7.093 ppm NaCl and a density of 1.019 g/cm^3 at 25°C. Brine-SF was used in experiments 1 and 2 performed with 3230S HPAM solutions. The brine-SW represented the seawater used in offshore polymer applications (Hatzignatiou *et al.,* 2013), its total dissolved solids content was 35.301 ppm and its density was 1.026 g/cm^3. Brine-SW was used in experiments 3 and 4, which involved 3630S HPAM solutions.

Table 2. Synthetic brines used for the preparation of the polymer solutions.

Brine Composition	San Francisco Field (SF) (ppm)	Sea Water (SW) (ppm)
NaCl	7.093	23.495
KCl	-	0.746
$MgCl_2$-$6H_2O$	-	9.149
$CaCl_2$-$2H_2O$	-	1.911
TDS (Total Dissolved Solids)	7.093	35.301

Source: Cortes *et al.,* 2016; Hatzignatiou *et al.,* 2013.

Tracer

Contained Salts in the brines acted as a tracer agent in all the experiments. Two brines were prepared as injection brines with 50% wt of the brine salinities in **Table 2**. For experiments 1 and 2, injection brine slug (brine S1) had a salinity of 3.547 ppm NaCl. For experiments 3 and 4, injected brine slug (brine S2) contained 17.651 ppm TDS.

Porous Media

Table 3 describes the Four different samples of consolidated Botucatu sandstones used in the experiments, each sample 100% water saturated. Typically, the Brazilian Botucatu formation is strongly water-wet and contains mainly fine-to-medium and well-selected quartz sandstones. The heterogeneity index of samples from the Botucatu formation are considered comparable with the Berea sandstones which are considered highly homogenous (Gomes, 1997). The average pore radius (r) for each Botucatu sample was determined by using **Eq. 1**, where is the absolute water permeability in square meters, and ϕ is the effective porosity in fraction. This equation is derived from the capillary bundle model of porous media. It combines Darcy´s law and Poiseuille´s Law (Zaitoun and Kohler, 1998).

$$r = \left(\frac{8k_w}{\phi}\right)^{1/2} \quad (1)$$

The samples were cleaned by the Soxhlet extraction method. To remove organic and inorganic particles, toluene and methanol were injected, and their petrophysical properties were determined according to API RP 40 (API, 1998).

Experimental Setup

In this study, the polymer concentration profile was determined by an ultraviolet light spectrophotometer. The UV and visible absorption spectra are measured by the attenuation of a beam light after it passes through a sample (in this case, the effluents of the experiments) at a specific wavelength. The Beer-Lambert Law states that the light attenuation of the spectrum is related to the properties of the crossed material by this light. The absorbance is proportional to the concentrations of the attenuating species in a sample. The inaccessible pore volume was determined by comparing the polymer profile with the corresponding salt (tracer) profile. The salt concentration profile was determined by the conductivity of the effluents. Inorganic salts contained in the brines acted as a tracer agent in all the experiments. Four retention tests were performed, all of them at constant flow rate of 1 mL/min at room temperature of 25°C. A schematic of the determination system of polymer retention is presented in **Fig. 1**. The bench is composed of storage cylinders for the injection fluids (1), pump (2), inlet capillary viscosimeter (3), core holder (4), capillary outlet viscosimeter (5), ultraviolet light spectrophotometer (6), conductivity meter (7), and digital balance (8).

Table 3. Petrophysical properties of the samples used in the experiments.

Sample	12A8	12A5	14cA2	14cA3
Diameter (cm)	3.72	3.72	3.78	3.76
Length (cm)	6.50	7.15	5.98	5.96
Pore Volume (cm3)	15.7	18.0	24.5	22.8
Dry Weight (g)	141.68	157.68	112.30	116.78
Average Pore Radius (μm)	3.39	3.51	13.1	11.6
Gas Permeability (mD)	320.6	358.4	7762	5823
Water Permeability (mD)	250.6	226.2	5001	5281
Porosity by gas - Boyle method (%)	22.2	23.2	36.5	34.5
Porosity by brine - Saturation method (%)	22.1	23.0	35.4	33.3
Difference between porosity methods (%)	0.51	0.99	3.11	3.45

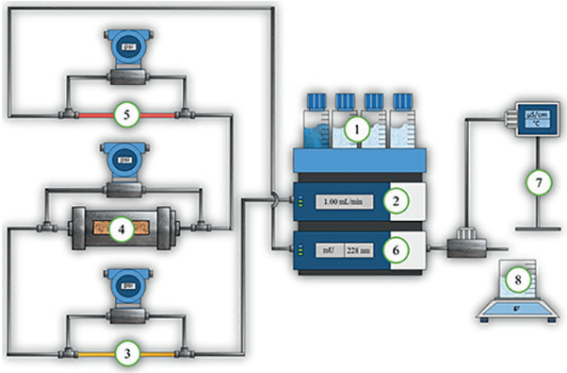

Fig. 1. Schematic of the polymer retention determination system.

Absorbance values for both polymer solutions were measured at different wavelengths aiming to define the detection limits for the ultraviolet light spectrophotometer. **Fig. 2** shows the polymer absorbance tendency as a function of wavelength for minimum and maximum concentration (100 ppm and 2000 ppm) for both polymers. At higher wavelengths than closely to 250nm, the equipment hardly detects the polymer molecules present in the solutions. Also at lower wavelengths than around 217 nm, the absorbance response exceeds the detectable limit (5 Absorbance Units) for 2000 ppm HPAM 3630S. Therefore, the optimal measurement range of the absorbance was defined between 0.171 (HPAM 3230S – 50ppm) and 1.02 (HPAM 3630S – 2000ppm) absorbance units. A wavelength of 228 nm was chosen for both polymers because at this wavelength, it is possible to detect the both polymers between the maximum and minimum concentrations without extrapolating the detection scale of the equipment.

Additionally, the behavior between the detected absorbance and the polymer concentration for both polymers (HPAM 3230S and 3630S) was determined (**Fig. 3**). This calibration process confirms that the absorbance response measured by the spectrophotometer and the polymer concentration of the polymer solutions has a linear relation and exits a direct proportionally to absorbance, avoiding any secondary effect related to the polymer concentration. The blue trend corresponds to HPAM 3230S and the orange trend belongs to HPAM 3630S. Their Pearson correlation coefficient R^2 was approximately 1, which means that it exits an almost perfect fit between observed and linear-modeled values. Also, Fig. 3 shows that HPAM 3630S presented higher absorbance values than absorbance values of the HPAM 3230S when they were compared at the same polymer concentration. It occurs due to the average molecular size differences.

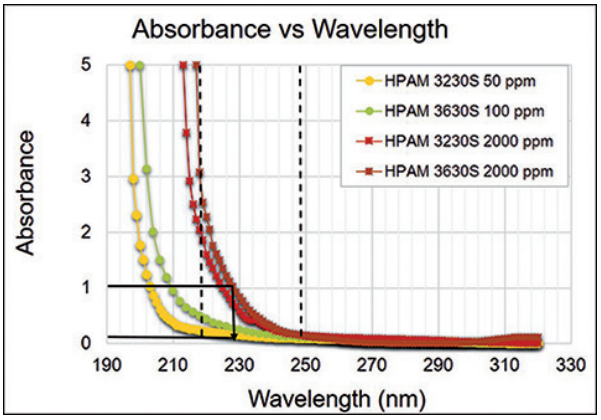

Fig. 2. Absorbance behavior as a function of the wavelength of the polymers.

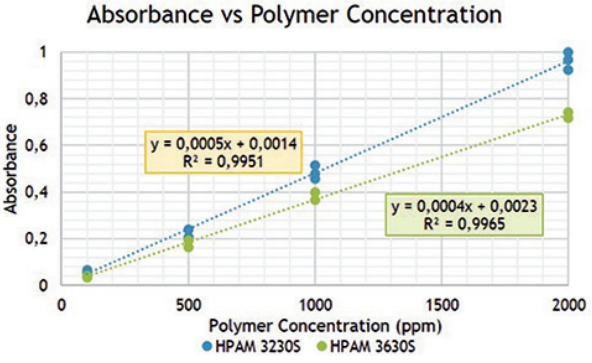

Fig. 3. Absorbance behavior as a function of polymer concentration for both polymers.

Dynamic Retention Measurement

The dynamic method applied in this study is based on the injection of two polymer banks separated by large pore volumes of brine injection (brine S1 and S2, according to the defined tracers). This experimental sequence allows determining the irreversible retention on porous media and the inaccessible pore volume (IPV). One polymer bank of 10 PV size is injected to establish an initial equilibrium of polymer retention. Successively, the irreversible retention is reached by the brine bank injection as post flush of 15 PV size (Ferreira and Moreno; 2017). Finally, assuming that no further retention and desorption occur, 10 PV polymer bank is injected so the inaccessible pore volume effect can be determined. Polymer retention can be quantified by the area difference between the polymer concentration profiles of the two polymer banks versus the injected pore volume (**Eq. 2**). Different authors as Lotsch *et al.* (1985), Hugues *et al.* (1990), Osterloh and Law (1998), Zhang and Seright (2014), Zhang and Seright (2015), Wan and Seright, 2016, Ferreira and Moreno (2017) have used this method successfully.

$$\Gamma = \frac{\sum_{i=1}^{n}\left[\frac{C_i}{C_o}2^{nd}bank - \frac{C_i}{C_o}1^{st}bank\right] * dPV * PV * \rho_{polymer} * C_o}{\rho_{rock} * V_{rock}} \quad (2)$$

Where, Γ is the polymer retention (µg/g), C_i is the polymer concentration in the effluents of each bank (ppm), C_o is the initial polymer concentration of each bank (ppm), dPV is a small step in pore volume normalized at each polymer concentration measurement, PV is the pore volume of the sample (cm^3), $\rho_{polymer}$ is the polymer solution density (g/cm^3), ρ_{rock} is the bulk rock density (g/cm^3) and V_{rock} is the volume of rock grains of the sample (cm^3).

On the other hand, resistance factor *(RF)* describes the effect of the mobility reduction by the water viscosity increase and the effective permeability decrease to the aqueous phase due to polymer addition (**Eq. 3**). It can be determined by differential pressure through the porous media at a constant flow rate of polymer (subscript *p*) and water (subscript *w*). (Bailjal, 1982).

$$RF = \frac{\lambda_w}{\lambda_p} = \frac{(\Delta p/q)_p}{(\Delta p/q)_w} \quad (3)$$

According to Rosa *et al.,* (2006), the residual resistance factor *(RRF)* describes the reduction of the effective permeability to water and is defined as the relation between the water mobility before (subscript *w*1) and after (subscript *w*2) the injection of the polymer solution (**Eq. 4**).

$$RRF = \frac{\lambda_{w1}}{\lambda_{w2}} = \frac{k_{w1}\mu_{w1}}{k_{w2}\mu_{w2}} = \frac{(\Delta p/q)_{w2}}{(\Delta p/q)_{w1}} \quad (4)$$

Additionally, the inaccessible pore volume could be calculated by **Eq. 5,** expresses the anticipation in the polymer propagation without any effect of polymer retention. For this reason, it was not calculated in the first polymer bank because there is a presence of both mechanisms. (Lotsch *et al.* 1985; Ferreira and Moreno, 2014). Eq. 5 takes into account the normalized pore volumes when occurs the polymer ($PV_{polymer}$) and the tracer (PV_{tracer}) breakthrough at 50-percent of the normalized concentration.

$$IPV = PV_{tracer} - PV_{polymer} \quad (5)$$

Injection Schemes

The two injection schemes were defined. Each one consisted of five HPAM banks at different concentrations. In the first, polymer banks are injected from the lowest to the highest concentration keeping the fundamental theory for the dynamic retention measurement (**Fig. 4**), while in the second scheme, polymer banks are injected from the highest to the lowest concentration (**Fig. 5**). The first brine bank was of 50 PV, to assure the cleaning of the samples. Consequently, each polymer bank injected was 20 PV and each brine bank was 30 PV. These schemes were designed for determining and quantifying the irreversible retention due to the first polymer bank (Eq. 2), the resistance factor (Eq. 3) and the absolute permeability reduction (Eq. 4) due to each polymer bank injected, and the inaccessible pore volume for the rock sample (Eq. 5). The 2000 ppm polymer bank was defined as the designed recovery polymer bank and the most diluted banks such as sacrifice banks. The defined nomenclature for polymer banks depends on their polymer concentration. The least concentrated bank in both schemes was called polymer bank C1 (concentration 01), and the most concentrated bank was named polymer bank C5 (concentration 05), for both injection schemes. Fig. 4 and Fig. 5 indicate the polymer bank C1 and C5 which correspond to 50 ppm and 2000 ppm, respectively.

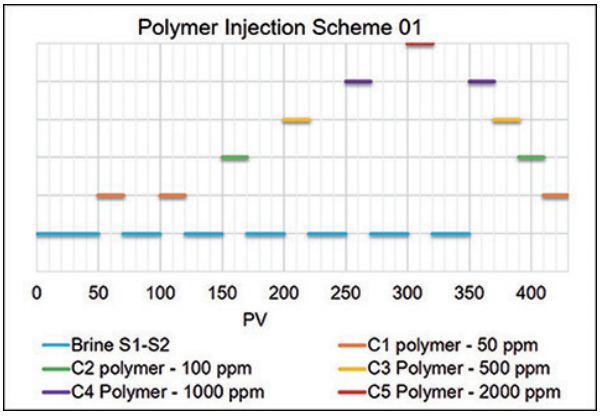

Fig. 4. Polymer injection type 01 – increasing polymer concentration scheme.

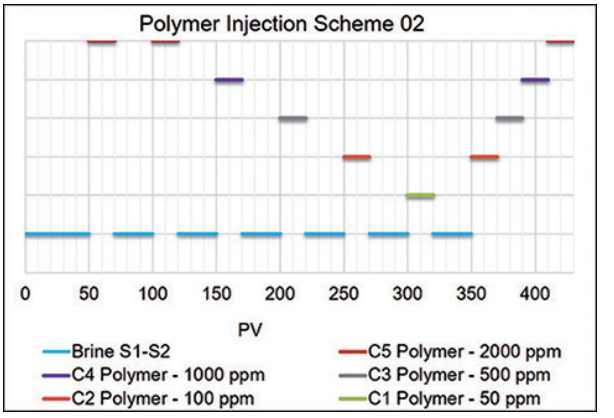

Fig. 5. Polymer injection type 02 – decreasing polymerconcentration scheme.

Results and Discussion

Polymer Rheology Behavior

The viscosity behavior of both polymers as a function of the polymer concentration and the shear rate was determined (**Fig. 6 and 7**). Each polymer was mixed with the correspondent brine to represent the San Francisco Field and an offshore prospect. Therefore, the HPAM 3230S and HPAM 3630S stock solutions were diluted with SF and SW brines, respectively. The viscosity of polymer dilutions from 50 ppm to 5000 ppm at shear rates varying from 0.1 s^{-1} up to 1000 s^{-1} was measured by a rheometer HAAKE MARS III at 25°C. As a reference, brine-SF and brine SW viscosities were 0.955 cP and 1.016 cP respectively at 7.848 s^{-1}. The IPT 83 mineral oil, with 200 cP at the test temperature, was used as a viscosity pattern for the rheometer aferition.

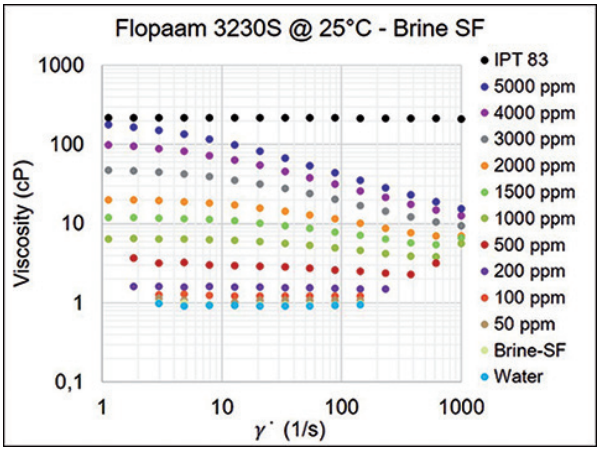

Fig. 6. HPAM Flopaam 3230S rheology in brine-SF.

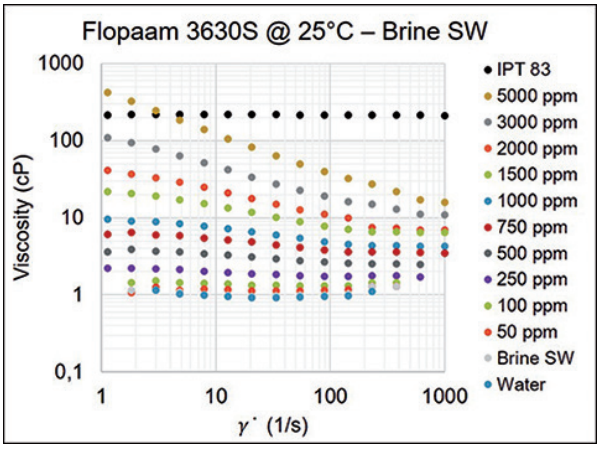

Fig. 7. HPAM Flopaam 3630S rheology in brine-SW.

Fig. 8 presents a comparative approach to the viscosity behavior of both polymers at a reference shear rate of 7.848 s^{-1}. Viscosity as a function of polymer concentration showed that HPAM 3630S was thicker than HPAM 3230S even under higher salinity conditions. The HPAM 3630s larger molecules balanced the adverse effects of the high salinity and the presence of divalent ions in the solution when compared to the HPAM 3230S molecules behavior.

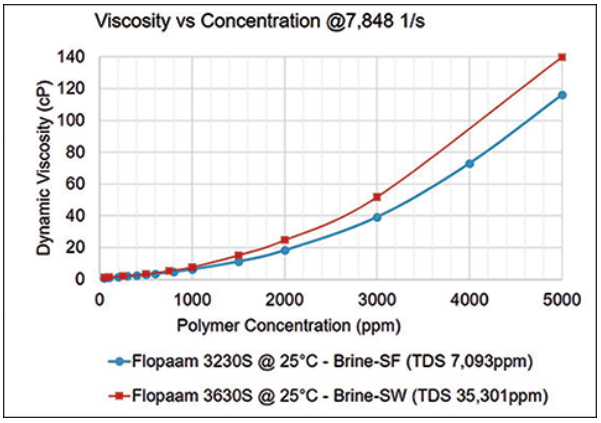

Fig. 8. Comparison between rheological behaviors for both polymers.

Al Hashmi *et al.,* (2013) determined the overlapping concentration (*C**) for a high-molecular weight HPAM by plotting the zero shear viscosity as a function of the polymer concentration. The log-log plot presents two distinct slopes at low and high concentrations. The overlap concentration is the concentration at the intersection of these two linear slopes. The overlapping concentration measures *C** the transition between the dilute and the semi-dilute regime for the pseudoplastic fluids. In the dilute regime, the molecules are separated from each other and they have an independent behavior. In the semi-dilute regime, the molecules are in contact with each other imposing friction. The transition between both regimes is characterized by a change in the tendency of the viscosity-concentration plot at a specific shear rate. **Fig. 9 and 10** show the overlapping concentration determined for HPAM 3230S and 3630S, respectively. The overlapping was detected at 700 ppm for HPAM 3230S, while for HPAM 3630S was noticed at 500 ppm. These results suggest that the overlapping concentration decreases as the molecular weight of the polymer increases.

The distance between the center of mass and one equivalent mass of the polymer molecule is called the radius gyration, is the parameter most widely used to characterize the polymers (FLORY, 1953). Assuming a polymer molecule as a body in constant movement due to the dynamic conditions present into the reservoir, it is necessary to calculate its weight-average radius of

gyration or hydrodynamic radius (R_g)to determine its molecular size.

$$C^* = \frac{M_w}{\frac{4}{3}\pi N_A R_g^3} \quad (6)$$

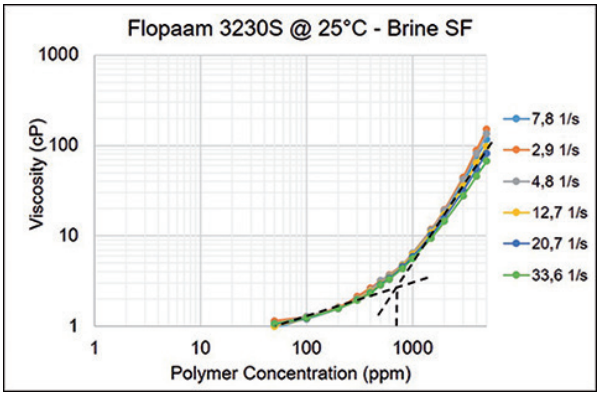

Fig. 9. Determination of the Overlapping Concentration for HPAM 3230S.

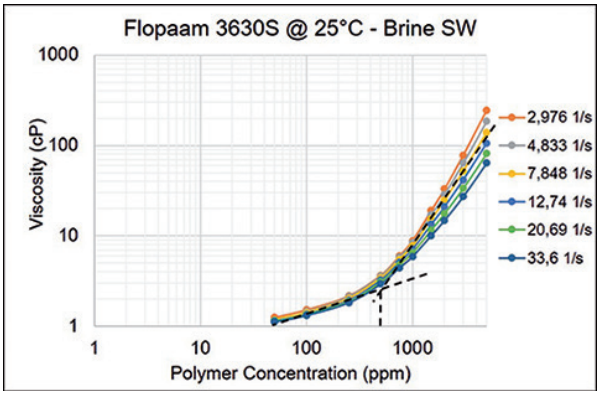

Fig. 10. Determination of the Overlapping Concentration for HPAM 3630S.

The radius of gyration of each polymer solutions was calculated using **Eq. 6**, where is the weight-average molar mass in mg/mole, N_A is 6.022x10^{23} in mole^{-1} (Avogadro's number), R_g is the radius of gyration in nanometer and C^* is the overlapping concentration in mg/nm^3 (BUCHHOLZ, 2003; AL HASHMI, 2013). A gyration radius of 150.3 nm to 165.4 nm was calculated for the HPAM 3230S solutions prepared with SF brine. That range corresponds to the molecular-weight range provided by the SNF Floerger company (6 – 8 million Daltons), and the overlapping concentration of 700 ppm detected previously. Likewise, for HPAM 3630S solutions in brine SW, a gyration radius of 251.2 nm was determined using the molecular weight of 20 million Daltons and the overlapping concentration of 500 ppm. **Table 4** summarizes the characterization results for both polymers used.

Dynamic retention tests

HPAM 3230S Experiments. Sandstone samples 12A8 and 12A5 were used for the retention experiments 1 and 2, performed with HPAM 3230S solutions, respectively. These samples were selected from their petrophysical similarities with the samples used in the previous retention works using the polymer HPAM 3230S (Zheng *et al.,* 2000; Zhang and Seright, 2014; Zhang and Seright, 2015; Wan and Seright, 2016; Chen *et al.,* 2016).

Table 4. Characterization Results of the Polymers.

HPAM Polymer/ Preparation Brine	Overlapping Concentration (ppm)	Radius of Gyration (nm)
3230S / Brine SF	700	150.3 - 165.4
3630S / Brine SW	500	251.2

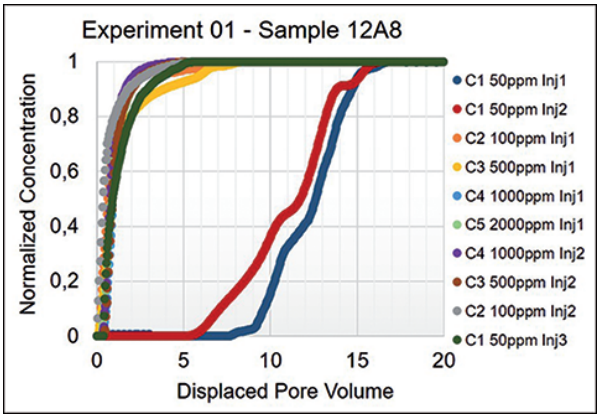

Fig. 11. Retention test 01 – Normalized concentration as a function of displaced pore volume in sample 12A8.

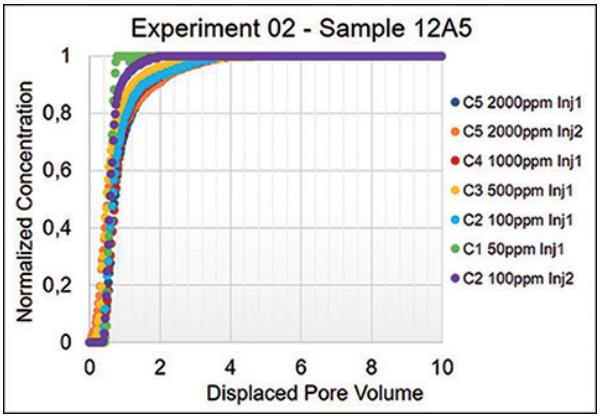

Fig. 12. Retention test 02 – Normalized concentration as a function of displaced pore volume in sample 12A5.

Fig. 11 shows the retention results of the experiment 01 in a plot of the normalized polymer concentration versus the displaced pore volume. The first polymer bank broke through around eight injected pore volumes. That breakthrough time indicates that the propagation and retention process of 50 ppm bank was slow. That extended retention period resulted as a consequence of the low polymer amount into the solution and the high retention capacity of the rock surface. Subsequent polymer banks of higher concentration than 50 ppm had satisfied the surface quickly, and their breakthrough occurred before 0.5 injected pore volumes. **Fig. 12** illustrates the retentions results of the experiment 02. All injected banks achieved the polymer breakthrough nearly 0.5 injected pore volumes. It could be concluded that polymer retention is strongly related to the average pore throat size of the samples, a faster polymer breakthrough in high pore throat size samples was observed.

Polymer Retention and Accumulated Polymer Retention

Using Eq. 2 and the results presented in Fig. 11 and 12, the amount of polymer retained due to each injected polymer bank was determined. The results for experiment 1 is presented in **Fig. 13**. Individual polymer retention cause by each polymer bank is represented by the blue column and the accumulated polymer retention or total amount of polymer retained during the experiment is illustrated by green column. An individual retention of 6.89 µg/g caused by 50 ppm polymer bank was obtained, while the recovery polymer bank of 2000 ppm experimented a retention of 6.70 µg/g. However, to achieve this individual retention for the 2000 ppm bank, cumulative polymer retention of 169 µg/g was induced by the sacrifice polymer banks injected previously to the recovery one. After that, the subsequently less concentrated banks did not contribute significantly to the accumulated polymer retention.

Fig. 14 illustrates the polymer retention results of the experiment 02. Initial polymer retention of 32.09 µg/g caused by the first 2000 ppm bank was measured. As shown in Fig. 13, at a particular polymer bank, an equilibrium in polymer retention is achieved, and after that, not significant additional retention is detected. Comparing the retention values for both 2000 ppm banks, 6.70 µg/g in the experiments 1 and 32,09 µg/g in the experiment 2, with and without sacrifice banks, polymer retention was reduced by 79.1%. Due to the low absolute permeability of the samples 12A8 and 12A5, a possible dominant retention mechanism was the mechanical entrapment in both cases. This statement can be supported by the higher accumulated retention value at the end of experiment 1. However, high values of polymer retention were induced in both experiments, and even using the sacrifice bank scheme, the cumulative polymer retention was higher (Fig. 13) than that initially injecting the more-concentrated polymer bank (Fig. 14). In this case, the use of the sacrifice bank is not recommendable because the HPAM 3230S proved not to be suitable for this type of absolute permeability.

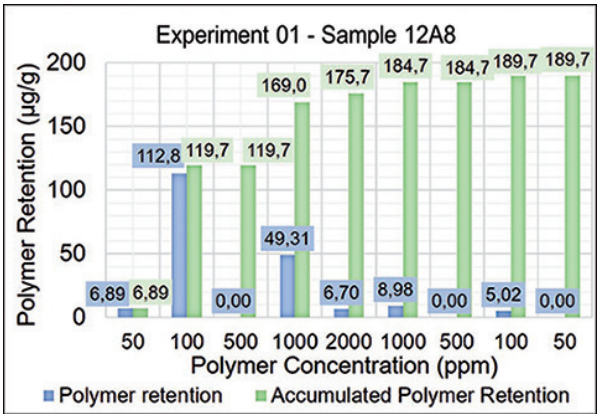

Fig. 13. Retention test 01 – Polymer retention results.

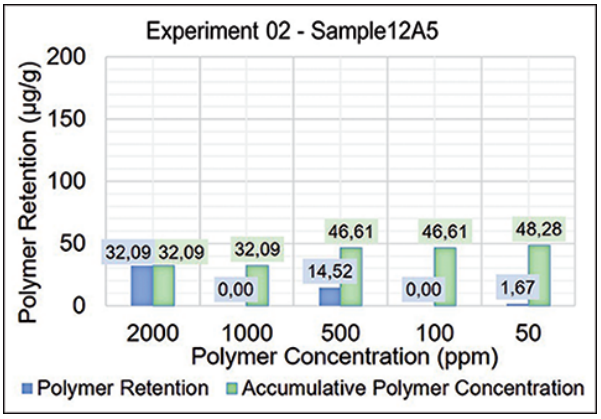

Fig. 14. Retention test 02 – Polymer retention results.

Inaccessible pore volume. **Fig. 15 and 16** present the values of inaccessible pore volume (IPV) for both experiments. The green line represents the normalized behavior of the polymer concentration effluents and the orange line corresponds to the normalized salt concentration present in the same injected polymer bank. In experiment 1 and 2, the C4 1000ppm Inj2 and C5 2000ppm Inj2 were selected for the IPV analysis, respectively. The calculated inaccessible pore volumes for experiments 1 (sample 12A8) and 2 (sample12A5) were 0.62 and 0.49 PV, respectively. These results imply that regardless of injected polymer concentration,

polymer did not contact 62% and 49% of the available pore volume in the Botucatu sandstone samples. That result is critical for the viability of the HPAM 3230S injection in samples of low permeability. The polymer banks would not sweep a significant amount of oil inside the porous media, even when this amount is high. One study by Pancharoen *et al.,* (2010) reported high IPV levels (33% to 49%) for high-molecular-weight polymer as HPAM 3630S, and established that the IPV dependency was a function of the polymer molecule size. This finding demonstrated the possibility to obtain high IPV levels using a larger polymer molecule as that of HPAM 3630S polymer.

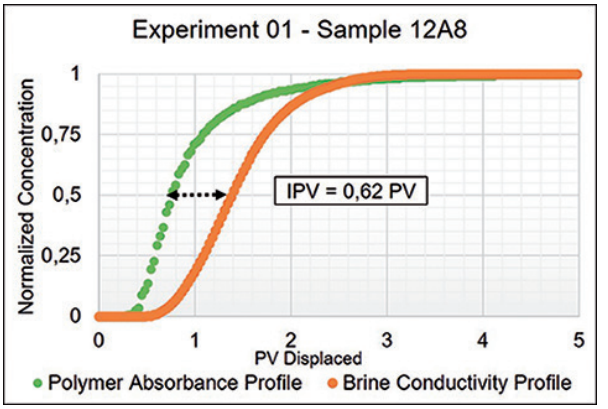

Fig. 15. Determinations of the inaccessible pore volume – Test 01.

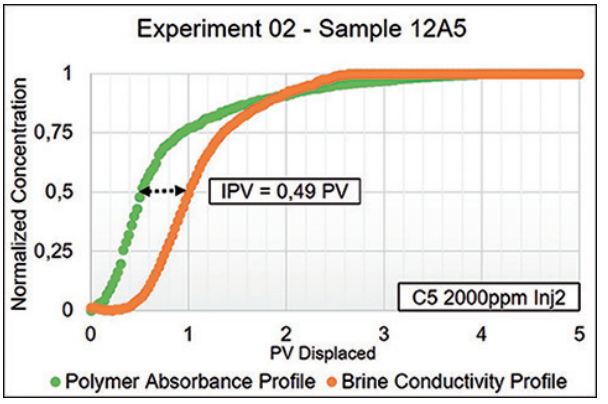

Fig. 16. Determinations of the inaccessible pore volume – Test 02.

Table 5 presents the comparison between the average pore radius of the sandstones samples used in both experiments and the gyration radius of the HPAM 3230S prepared with the brine SF. According to these results, the available pore space is larger than the calculated size of the polymer molecule. From the ratio r/R_g, It was determined the pore size as 22.6 and 23.4 times larger than the molecular polymer size. These results could explain why some polymer molecules did get into the samples. It is worth point out that the values included in Table 5 represent average values. Therefore, smaller and larger pores probably exist filtering some polymer molecules and causing mechanical trapping. It might also explain why some polymer molecules could not access part of the pores, which is also confirmed by the IPV results.

From the IPV results, it can be concluded that the HPAM 3230S molecule is considerably larger than most of the pores in both samples. That statement implies that the polymer in field applications under similar petrophysical conditions would contact a significant amount of oil. Also, once the IPV behavior is a function of the ratio between polymer size and pore throat size, the HPAM 3230S probably should be used in a polymer-flooding process through a more permeable porous media, avoiding the high retention levels as obtained in experiments 1 and 2.

Table 5. Comparison between Average Pore Radius of the Sandstones and the Radius of Gyration of the HPAM 3230S.

	Average Pore Radius (µm)		IPV (% PV)
Sample 12A8	3.39	22.6	62
Sample 12A5	3.51	23.4	49
Radius of Gyration (µm)			
HPAM 3230S	0.150	-	-

Residual Resistance Factor and Resistance Factor Behaviors

Fig. 17 and 18 present the residual resistance factors (RRF) and resistance factors (RF) results for each of the injected banks in Experiments 1 and 2, correspondingly. These values were calculated based on the Eq. 3 and 4 for experiments at a constant flow rate. The highest RRF values were detected in the first polymer bank in both experiments (11.72 and 3.32 in experiment 1 and 2, respectively). These results evidence the significant impact that the first bank has in absolute permeability in porous media without previous polymer contact. The subsequently injected banks did not significantly affect the RRF. The highest values of RRF were detected at the first polymer banks injected regardless of its concentration (blue columns in Fig. 17 and 18). Thus RRF values begin to be relatively constant when the accumulated retention is also constant.

In the case of the resistance factor, the highest value in both experiments was detected at the highest concentration bank, as expected. In test 01, 2000 ppm bank generated a value of 31.64 and in experiment 02,

the 2000 ppm banks caused values of 21.07 and 24.89. This demonstrates the resistance factor dependence on the polymer concentration or polymer solution viscosity. Comparing the resistance factors between 2000 ppm banks in both tests allow to conclude that in experiment 01, the target 2000 ppm bank suffered lower retention than in experiment 02, caused by the smaller viscosity reduction in experiment 01.

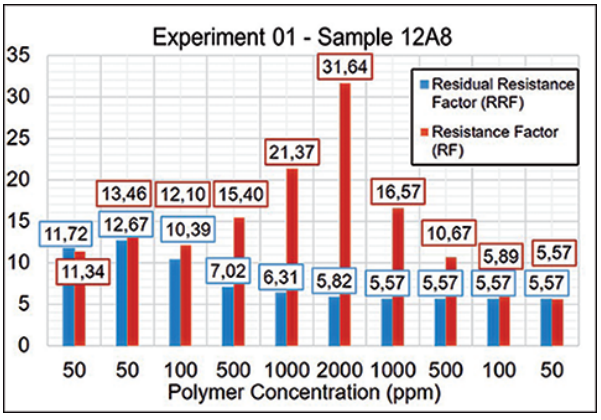

Fig. 17. Retention test 01 – Polymer retention results.

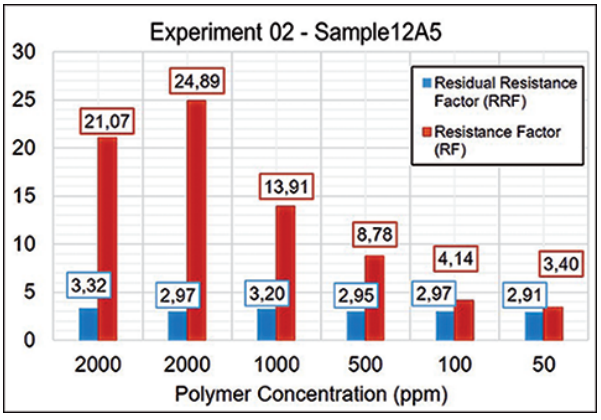

Fig. 18. Retention test 02 – Polymer retention results.

Fig. 19 and 20 present complementary results of residual resistance factors (RRF) for both tests. The reduction performances of the absolute permeability as a function of the displaced pore volume for both experiments were plotted. By measuring the differential pressure at steady state flow of the injected brine after each polymer bank, the absolute permeability reduction was quantified. After the 50 ppm flooding in Fig. 19, the original value reduced by 8.5% of the initial permeability. On the other hand, once 2000 ppm bank was injected, the absolute permeability decreased by 30.1% of the initial value (Fig. 20). These results showed that it does not exist a linear relation between the permeability reduction and the polymer concentration value. Additionally, after the injection of the 500 ppm bank in experiment 1, a slight permeability restoration was observed (Fig. 17). In this case, the permeability reduction goes from 8.5% to 18% of its original value. That could occur because of an actual pore reduction due to the polymer retention in the rock sample. A smaller pore space leads to an increase of the linear velocity, which can remove polymer particles. That is a well-known phenomenon of formation damage experiments due to organic scales (Ali and Islam, 1988; Carrillo *et al.,* 2014).

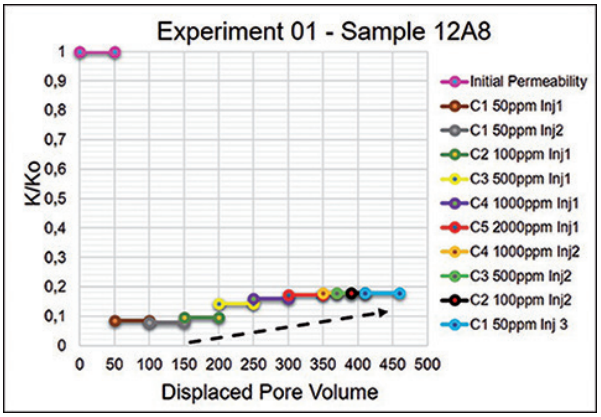

Fig. 19. Reduction of absolute permeability due to each polymer bank – Test 01.

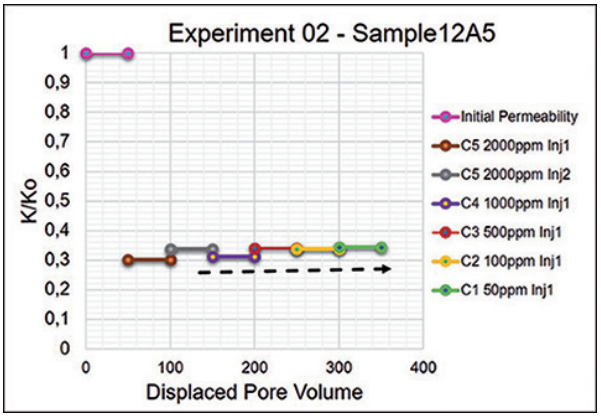

Fig. 20. Reduction of absolute permeability due to each polymer bank – Test 02.

HPAM 3630S Experiments

Chen *et al.,* (2016) reported a survey of the influencing factors on polymer hydrodynamic retention using several polymers of different molecular weights including the HPAM 3630S. Nevertheless, according to our knowledge, experimental studies about HPAM 3630S retention and its polymer concentration dependence has not been published. The following results relate to the samples 14cA2 and 14cA3, used in experiments 03 and 04, respectively, and HPAM 3630S prepared with the brine-SW. The brine S2 was used as the tracer in

both experiments. To avoid measurement and analyzing problems with absorbance presented in experiment 1 with the 50ppm polymer banks (Fig. 11), it was decided to perform experiments 3 and 4 without these polymer banks. Therefore, the initial polymer bank (C1 polymer bank) in experiment 3 corresponds to 100ppm polymer bank. In spite of this modification, the injection schemes used in experiments 3 and 4 preserved their injection order, as was defined in Fig. 4 and 5. HPAM 3630S experiments had the same data analysis of the HPAM 3230S experiments.

For experiments 3 and 4, the absorbance behavior as function of the displaced pore volume was normalized and the corresponding results are presented in **Fig. 21 and 22**, respectively. These results showed that all injected polymer banks presented a breakthrough at less than one displaced pore volume. However, the first polymer bank (C1 100ppm Inj1) presented a slow retention process into the porous media despite the fast polymer solution propagation in Fig. 21. This phenomenon was also identified in experiment 1 (Fig. 11) in its first polymer bank injected (C1 50ppm Inj1).

Polymer Retention and Accumulated Polymer Retention

From Fig. 21 and 22 results and using Eq. 2, the retained polymer caused by each injected polymer bank could be calculated. Fig. 23 and 24 summarize the polymer retention results in both experiments. In experiment 3, the first (C1 100ppm) and the second (C2 500 ppm) polymer bank only caused the polymer retention, with values of 39.15 µg/g and 19.7 µg/g, respectively (Fig. 23). The following injected banks did not generate any additional polymer retention, and the 1000 ppm and 2000 ppm banks kept its dynamic viscosity (which was the purpose of the injection of the sacrifice bank). In the same manner, by changing the injection scheme in Fig. 24, the first (C4 2000ppm) and the second (C3 1000ppm) polymer bank only caused the polymer retention, with values of 72.01 µg/g and 26.24 µg/g, correspondingly. After that, the succeeding injected banks did not contribute to these retention values, as occurred in experiment 3. The comparison between the retention results of target 2000 ppm bank in experiments 3 and 4 validated the initial hypothesis regarding to the injection of a sacrifice polymer bank and its effect on polymer retention.

There was no loss of polymer mass for the more concentrated bank in Fig. 24. In this case, the efficiency of the sacrifice bank was 100% compared with the polymer retention induced only by 2000-ppm polymer bank. However, to achieve this result was induced cumulative polymer retention of 58.9 µg/g caused by the initial sacrifice polymer banks, which represents a 19% of retention reduction. After that, the subsequently injected banks did not contribute significantly to the accumulated polymer retention.

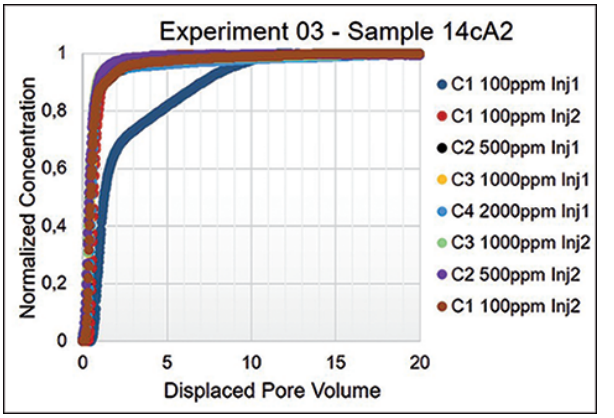

Fig. 21. Retention test 03 – Normalized concentration as a function of displaced pore volume in sample 14cA2.

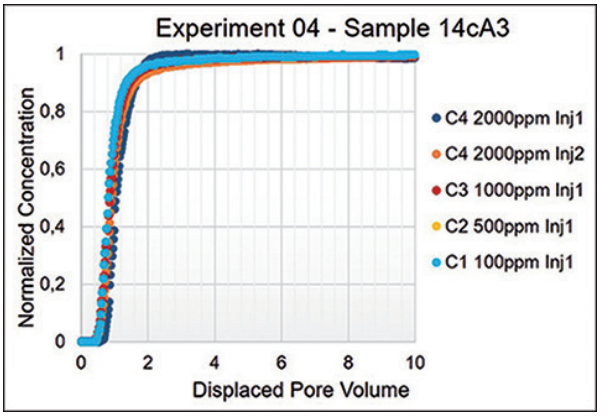

Fig. 22. Retention test 04 – Normalized concentration as a function of displaced pore volume in sample 14cA3.

Inaccessible pore volume

Fig. 25 and 26 show normalized polymer concentration as a function of the injected pore volume, which allows determining the inaccessible pore volume for both samples 14cA2 and 14cA3. The blue line represents the breakthrough behavior of the polymer bank (with the retention effect) and the red line corresponds to the breakthrough tendency of the salt present in the polymer bank. In experiments 3 and 4, the C1 100ppm Inj2 and C4 2000ppm Inj2 were selected for the IPV calculation, respectively. In these cases, 0.25 and 0.23 PV were calculated as IPV. These results are consistent with

previous developed studies, which report values are between 0.1 and 0.3 pore volumes (Dawson and Lantz, 1972; Szabo, 1975; Gupta, 1978; Lotsch *et al.,* 1985; Huh *et al.,* 1990; Hughes *et al.,* 1990; Mezzomo *et al.,* 2002; Pancharoen *et al.,* 2010; Hatzignatiou *et al.,* 2013; Ferreira and Moreno; 2017). It probably means that the inaccessible pore volume for the high-permeability samples presented a reasonable value according to the literature and the HPAM 3630S is well-selected for this high-permeability range.

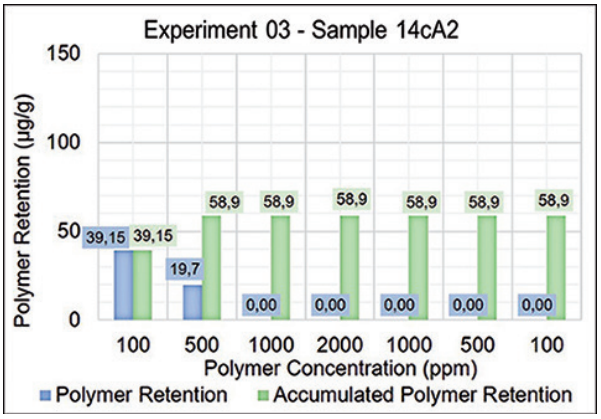

Fig. 23. Results of the retention test 03.

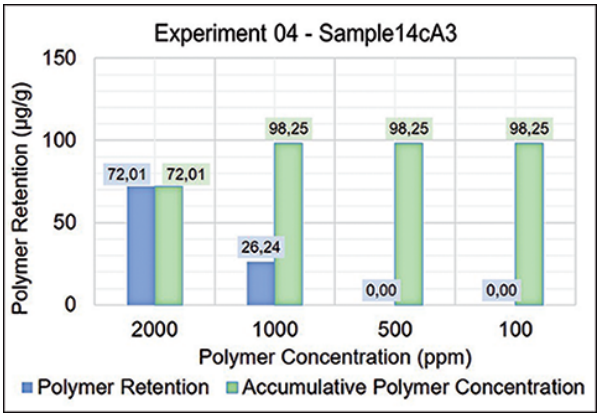

Fig. 24. Results of the retention test 04.

Table 6 presents the comparison between the average pore radius of the sandstones samples used in experiments 3 and 4, and the radius of gyration of the polymer solution of HPAM 3630S prepared in brine SW. As concluded for HPAM 3230S experiments, the average pore radius of 14cA2 and 14cA3 samples is larger than the radius of gyration of HPAM 3630S. The pore size is 52.16 and 46.4 times larger than the polymer molecule size.

In all cases including HPAM 3230S and HPAM 3630S experiments, the average pore radius always was larger than the radius of gyration of the polymer molecule, which means that in all cases polymer solution did get into the samples. However, the parameter r/R_g, which measures the size differences between the pore and the polymer, are higher (52.1 and 46.4) for HPAM 3630S experiments than those in HPAM 3230S experiments (22.6 and 23.4). Besides, the lower IPV values (0.25 and 0.23) were calculated at the higher r/R_g values. This finding suggests that exits a relationship between the IPV and the parameter r/R_g.

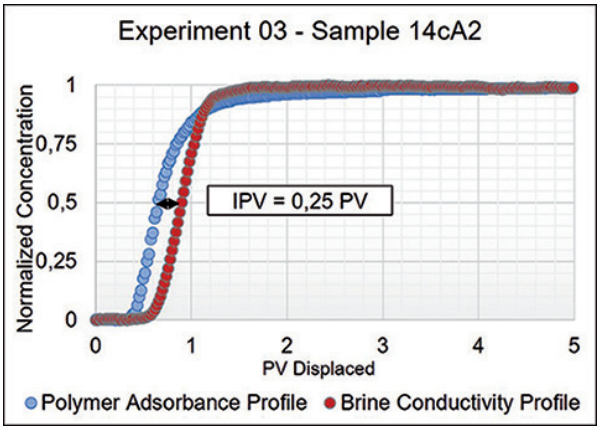

Fig. 25. Determinations of the inaccessible pore volume – Test 03.

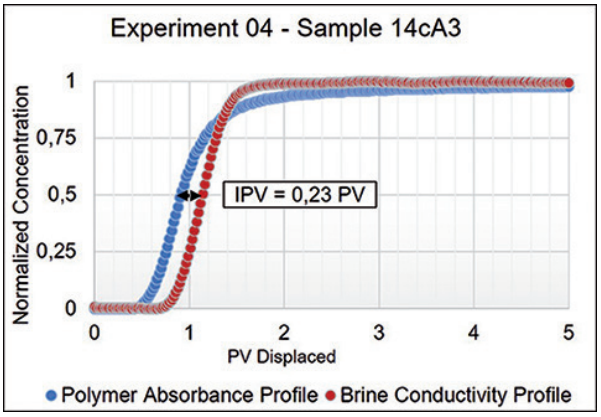

Fig. 26. Determinations of the inaccessible pore volume – Test 04.

Table 6. Comparison between Average Pore Radius of the Sandstones and the Radius of Gyration of the HPAM 3630S.

	Average Pore Radius (µm)		IPV (% PV)
Sample 14cA2	13.04	52.1	25
Sample 14cA3	11.62	46.4	23
Radius of Gyration (µm)			
HPAM 3630S	0.251	-	-

Residual Resistance Factor and Resistance Factor Behaviors

As concluded for the HPAM 3230S case, experiments 03 and 04 presented a similar trend for the resistance factor (**Fig. 27 and 28**). Furthermore, the efficiency of the mobility reduction in these results was evidenced. Lower values of residual resistance factor were obtained for HPAM 3630S experiments than for HPAM 3230S ones. Pointed out the high absolute permeability of the sandstones samples and polymer molecule size used in experiments 03 and 04, the permeability reduction was not critical as in experiments 01 and 02. The residual resistance factor (RRF) was increasing while the polymer banks were injected into the porous media independent on their polymer concentration in both 3630S experiments.

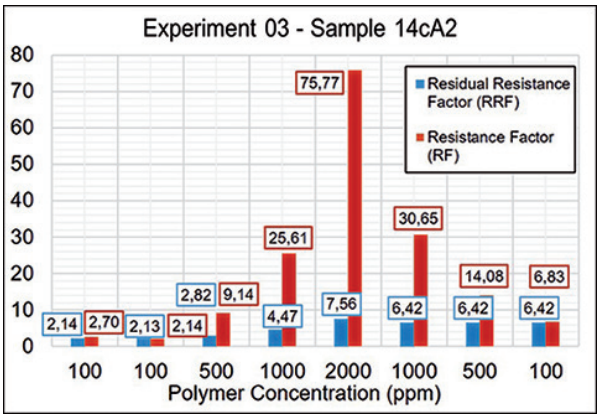

Fig. 27. Retention test 03 – Polymer retention results.

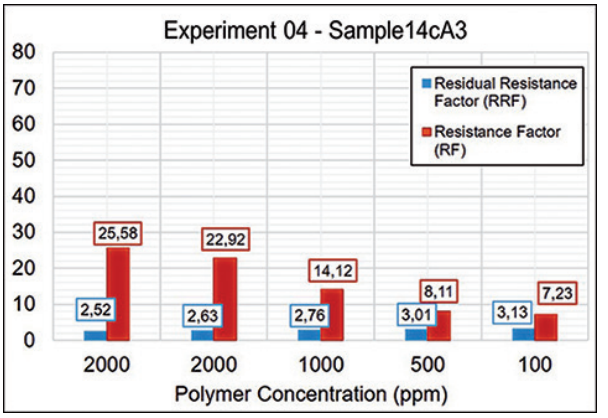

Fig. 28. Retention test 04 – Polymer retention results.

Fig. 29 and 30 present the permeability reduction behavior caused by each polymer bank injected in both 3630S experiments. Also, as commented for HPAM 3230S experiments, the first polymer banks produced the highest reduction, 46.6% and 39.3% for samples 14cA2 and 14cA3, respectively. Then, the final permeability reduction was achieved with values of 15.5% and 31.9 %, correspondingly. As shown in Fig. 27 and 28, the permeability reduction process due to polymer retention of the injected solutions is a phenomenon that is not related to their polymer concentration into the flooding solution. These results proved that the permeability reduction occurs as a gradual process without drastic changes in its tendency until achieving the final permeability reduction.

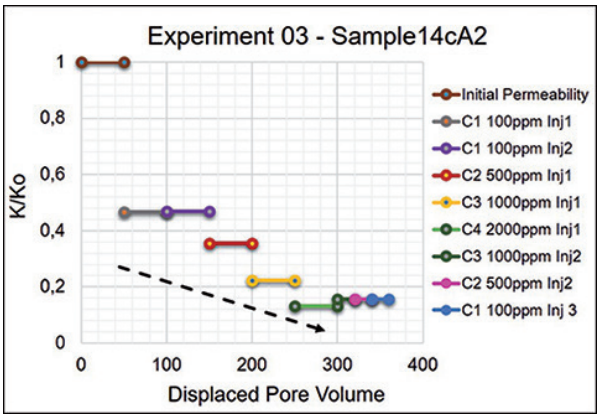

Fig. 29. Reduction of absolute permeability due to each polymer bank – Test 03.

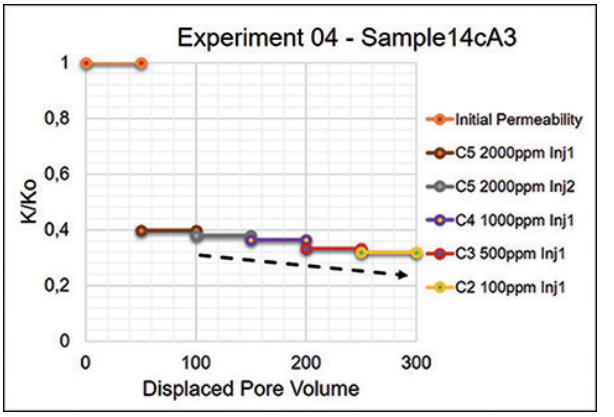

Fig. 30. Reduction of absolute permeability due to each polymer bank – Test 04.

Conclusions

For the tested conditions, the injection of the sacrifice polymer bank reduced the polymer retention. The retention of 2000ppm bank for HPAM 3230S was reduced by 79%. For HPAM 3630S tests, an individual 2000ppm bank did not experiment polymer retention due to previous injected sacrifice banks. However, an amount of polymer was initially lost into the porous media to achieve this reduced retention, which reflects in accumulative retention values; a cumulative retention of 175.7 µg/g was observed for the HPAM 3230S case

and 58.9 µg/g for HPAM 3630S case. This cumulative retention values mean the polymer amount that porous media requires to saturate itself and avoid polymer retention process.

In experiments 1 and 3, the first injected bank (less concentrated) exhibited some unexpected behaviors. The breakthrough for the 50ppm bank occurred around eight injected pore volumes (3230S HPAM experiment). However, the 100ppm bank broke through after less than one displaced pore volume (3630S HPAM experiment). This comparison suggests the existence of different retention mechanisms in both tests. In the first test, chemical adsorption and mechanical entrapment were presented, it could be explained by high polymer retention and low velocity for polymer breakthrough as shown in Fig. 15. In the second one, only the chemical adsorption mechanism was evidenced, because there was a quick propagation of polymer bank and there was no interference evidence in Fig. 25.

The absolute permeability reduction process did not have a linear trend with the polymer concentration of the injected solutions. This statement was confirmed by all retention experiments conducted. Furthermore, results suggested that the permeability reduction is probably a phenomenon strongly dependent on the retention mechanisms involved. The first polymer injection regardless of its concentration affected more the porous media permeability than the subsequently injected banks. Also, two different trends of permeability reduction were identified. The first trend (HPAM 3230S experiment) is a typical reduction in low-permeability samples whose main feature is the partial restoration of the permeability, and the second one (HPAM 3630S experiment) is a representative behavior in high-permeability samples, which the main characteristic was a gradual decrease of the permeability.

The inaccessible pore volume (IPV) presented an evident dependence on the ratio between the average pore radius and the radius of gyration of the polymer. Although the radius of gyration of both polymers was smaller than the average pore radius, an inverse relationship between these parameters was observed, i. e., higher IPV was obtained at lower ratios. Taking into account the pore size distribution around the average value, higher IPV (HPAM 3230S experiments) can be probably attached to the mechanical entrapment mechanism caused by the smaller pores. Therefore, is advisable to use the HPAM 3230S in more permeable porous media. Although typical IPV values were calculated for HPAM 3630S, the mechanical entrapment was avoided due to the high permeability of the samples.

The rheology results for both polymers evidenced that HPAM 3630S was thicker than HPAM 3230S even under higher salinity conditions. An explanation is the molecular weight differences between both polymers. HPAM 3630S molecules are larger than HPAM 3230S, giving to them a higher viscosifyng capacity, balancing the adverse effect of the high salinity and even in the presence of divalent ions in the solution when they are compared to the HPAM 3230S molecules behavior.

Acknowledgement

The authors would like to thank Laboratory of Oil Reservoirs at Unicamp (LABORE), the Energy Department at School of Mechanical Engineering (FEM), Coordination for the Improvement of Higher Education Personnel (CAPES) and Organization of American States (OAS) and the Coimbra Group of Brazilian Universities (GCUB) for their financial support.

Nomenclature

$(\Delta p)_w$	=	Differential pressure of brine bank at steady state, psi.
$(\Delta p)_p$	=	Differential pressure of polymer bank at steady state, psi.
$(\Delta p)_{w1}$	=	Differential pressure before polymer bank injection at steady state, psi.
$(\Delta p)_{w2}$	=	Differential pressure after polymer bank injection at steady state, psi.
C^*	=	Overlapping concentration, ppm.
C_i	=	Polymer concentration in the effluents of each bank, ppm.
C_o	=	Initial polymer concentration of each bank, ppm.
N_A	=	Avogadro's number (6.022×10^{23}), $mole^{-1}$.
$PV_{polymer}$	=	Normalized pore volume where occurred the polymer breakthrough, PV.
PV_{tracer}	=	Normalized pore volume where occurred the tracer breakthrough, PV.
R_g	=	Radius of gyration, nm.
V_{rock}	=	Volume of rock grains, cm^3.
λ_p	=	Polymer mobility.
M_w	=	Weight-average molar mass (mg/mole).
K_w	=	Absolute Water Permeability (cm^2).
λ_w	=	Water mobility.
$\rho_{polymer}$	=	Polymer solution density, g/cm^3.
ρ_{rock}	=	Bulk rock density, g/cm^3.

dPV = Differential of pore volume normalized.
μ = Dynamic viscosity, cP.
IPV = Inaccessible pore volume.
K/K_o = Absolute permeability reduction.
PV = Pore volume, cm^3.
RF = Resistance factor.
RRF = Residual resistance factor.
q = Flow rate, cm^3/min.
r = Average pore radius, µm.
Γ = Polymer retention, µg polymer/g rock.
λ = Mobility.
ϕ = Effective porosity.

References

Al Hashmi, A. R.; Al Maamari, R. S.; Al Shabibi, I. S.; Mansoor, A. M.; Zaitoun, A.; Al Sharji, H. H. Rheology and mechanical degradation of high-molecular-weight partially hydrolyzed polyacrylamide during flow through capillaries. Journal of Petroleum Science and Engineering, v. 105, p. 100-106, 2013.

Ali, M. A.; Islam, M. R. The effect of asphaltene precipitation on carbonate-rock permeability: an experimental and numerical approach. SPE production & facilities, v. 13, n. 03, p. 178-183, 1998.

Api, R. P. Recommended Practices for Core Analysis 40. 1. ed. Washington, DC: American Petroleum Institute, 1998.

Api, R. P. Recommended Practices for Evaluation of Polymers Used in Enhanced Oil Recovery Operations 63. 1. ed. Washington, DC: American Petroleum Institute, 1990. v.1.

Araujo, Y. C., & Araujo, M. (2018). Polymers for application in high temperature and high salinity reservoirs–critical review of properties and aspects to consider for laboratory screening. *Fuentes: El reventón energético*, *16*(2), 55-71.

ASTM. Standard Specification for Reagent Water D1193-06. ASTM International, West Conshohocken, PA, 2011.

Aya, C. L. D., Guardia, V. M. D., Toro, G. A. M., García, R. H. C., & Pérez, H. I. Q. (2018). Metodología para la priorización de tecnologías emergentes de recobro mejorado químico. *Revista Fuentes*, *16*(2).

Baijal, S.K. Flow Behaviour of Polymers in Porous Media. Tulsa, Oklahoma: PennWell Publishing Company, 1982.

BP Group. BP statistical review of world energy. BP World Energy Review, 2015.

Broseta, D.; Medjahed, F.; Lecourtier, J.; Robin, M. Polymer Adsorption/Retention in porous media: Effects of core wettability on residual oil. SPE Advanced Technology Series, v. 3, n. 01, p. 103-112, 1995.

Buchholz, B. A.; Zahn, J. M.; Kenward, M.; Slater, G. W.; Barron, A. E. Flow-induced chain scission as a physical route to narrowly distributed, high molar mass polymers. Polymer, v. 45, n. 4, p. 1223-1234, 2004.

Carrillo, L. F.; Ariza Leon, E.; Padron, R.; Lizcano, J. Evaluation of the Effect of the Asphaltene Accumulation in Porous Media at Dynamic Conditions for a Colombian Crude Oil. In: SPE Heavy And Extra Heavy Oil Conference: Latin America. Society Of Petroleum Engineers, 2014, Medellin. Proceedings…Medellin: Society of Petroleum Engineers, 2014.

Chen, T. R.; Chen, Z. Multiphase physicochemical flow in porous media and measurement of relative permeability curves. Fundamentals and Advances in Combined Chemical Flooding. China Petrochemical Press, Beijing, 2002.

Chen, Z.; Du, C.; Kurnia, I.; Lou, J.; Zhang, G.; Yu, J.; Lee, R. L. A Study of Factors Influencing Polymer Hydrodynamic Retention in Porous Media. IN: SPE IMPROVED OIL RECOVERY CONFERENCE, 2016, Tulsa. Proceedings… Tulsa: Society of Petroleum Engineers, 2016.

Cortes, J. E.; Muñoz, L. F.; Gonzalez, C. A.; Niño, J. E.; Polo, A.; Suspes, A.; Trujillo, H. Hydrogeochemistry of the formation waters in the San Francisco field, UMV basin, Colombia–A multivariate statistical approach. Journal of Hydrology, v. 539, p. 113-124, 2016.

Dawson, R.; Lantz, R. B. Inaccessible pore volume in polymer flooding. Society of Petroleum Engineers Journal, v. 12, n. 05, p. 448-452, 1972.

Ferreira, V. H. S.; Moreno, R. B. Z. L. Impact of flow rate variation in dynamic properties of a terpolymer in sandstone. Journal of Petroleum Science and Engineering, v. 157, p. 737-746, 2017.

Flory, Paul J. Principles of polymer chemistry. Cornell University Press, 1953.

Gogarty, W. B. Mobility control with polymer solutions. Society of Petroleum Engineers Journal, v. 7, n. 02, p. 161-173, 1967.

Gomes, J. A. T. Visualização e Análise do Deslocamento Imiscível e Instável em Meio

Poroso Consolidado. Universidade Estadual de Campinas (UNICAMP), Faculdade de Engenharia Mecânica, Campinas - São Paulo: Tese (Doutorado em Ciência e Engenharia de Petróleo), 1997.

Green, D. W.; Willhite, G. P. Enhanced oil recovery; Henry L. Doherty Memorial Fund of AIME. Society of Petroleum Engineers: Richardson, TX, 1998.

Hatzignatiou, D. G.; Moradi, H.; Stavland, A. Experimental investigation of polymer flow through water-and oil-wet Berea sandstone core samples. In: Eage Annual Conference & Exhibition Incorporating SPE Europec, 2013, London. Proceedings…London: Society of Petroleum Engineers, 2013.

Hernandez, F. A. T., Niño, J. C. L., & Moreno, R. L. (2018). Effects of salts and temperature on rheological and viscoelastic behavior of low molecular weight HPAM solutions. *Revista Fuentes*, *16*(1), 19-35.

Hughes, D. S.; Teeuw, D.; Cottrell, C. W.; Tollas, J. M. Appraisal of the use of polymer injection to suppress aquifer influx and to improve volumetric sweep in a viscous oil reservoir. SPE Reservoir Engineering, v. 5, n. 01, p. 33-40, 1990.

Huh, C.; Lange, E. A.; Cannella, W. J. Polymer retention in porous media. In: SPE/DOE Enhanced Oil Recovery Symposium, 1990, Tulsa. Proceedings…Tulsa: Society of Petroleum Engineers, 1990.

Lotsch, T.; Muller, T.; Pusch, G. The effect of inaccessible pore volume on polymer coreflood experiments. In: SPE Oilfield and geothermal chemistry symposium, 1985, Phoenix. Proceedings… Phoenix: Society of Petroleum Engineers, 1985.

Mezzomo, R. F.; Moczydlower, P.; Sanmartin, A. N.; Araujo, C. H. V. A new approach to the determination of polymer concentration in reservoir rock adsorption tests. In: SPE/DOE Improved Oil Recovery Symposium. Society Of Petroleum Engineers, 2002, Tulsa. Proceedings…Tulsa: Society of Petroleum Engineers, 2002.

Molano, A. M. J., Navarro, S. F. M., & Díaz, R. J. (2014). Metodología para el diseño de baches en un proceso de inyección de polímeros para recobro mejorado, considerando fenómenos de interacción roca/fluidos. *Fuentes: El reventón energético*, *12*(2), 6.

OPEC. Annual Report 2017 - Organization of the Petroleum Exporting Countries, 2017. Vienna, Austria, 2017. ISSN 0475-0608.

Osterloh, W. T.; Law, E. J. Polymer Transport and Rheological Properties for Polymer Flooding in the North Sea. IN: SPE/DOE IMPROVED OIL RECOVERY SYMPOSIUM, 1998, Tulsa. Proceedings…Tulsa: Society of Petroleum Engineers, 1998.

Pancharoen, M.; Thiele, M. R.; Kovscek, A. R. Inaccessible pore volume of associative polymer floods. In: SPE IMPROVED OIL RECOVERY SYMPOSIUM, 2010, Tulsa. Proceedings…Tulsa: Society of Petroleum Engineers, 2010.

Pinto, M. S., Herrera, D. M., & Angarita, J. C. G. (2018). Production optimization for a conceptual model through combined use of polymer flooding and intelligent well technology under uncertainties. *Revista Fuentes*, *16*(1), 37-45.

Rosa, A. J.; De Souza Carvalho, R.; Xavier, José Augusto Daniel. Engenharia de reservatórios de petróleo. Interciência, 2006.

Sheng, James. Modern chemical enhanced oil recovery: theory and practice. Gulf Professional Publishing, 2010.

SNF Floerger. In "Enhancing Polymer Flooding Performance 30 Years of Experience in EOR". 2014. Disponível em: <http://snf.us/wp-content/uploads/2014/08/EOR-Oil-30-Years-of-EOR1.pdf>. Acesso em: January 10, 2018.

SORBIE, K. S. Polymer-improved Oil Recovery, CRC Press, Inc. USA and Canada. 1991.

Sun, G., Crouse, B., Freed, D. M., Xu, R., Bautista, J., Zhang, R., ... & Dressler, M. (2018). Polymer flooding–Does Microscopic Displacement Efficiency Matter?. *Revista Fuentes*, 16(2).

SZABO, M. T. An evaluation of water-soluble polymers for secondary oil Recovery-Parts 1 and 2. Journal of Petroleum Technology, v. 31, n. 05, p. 553-570, 1979.

SZABO, M. T. Some aspects of polymer retention in porous media using a C14-tagged hydrolyzed polyacrylamide. Society of Petroleum Engineers Journal, v. 15, n. 04, p. 323-337, 1975.

Toro, G. M., Herrera, J. J., Orrego, J. A., Rojas, F. A., Rueda, M. F., & Manrique, E. J. (2018). Effect of ionic composition in water: oil interactions in adjusted brine chemistry waterflooding: preliminary results. *Fuentes: El reventón energético*, *16*(2), 73-82.

Vela, S.; Peaceman, D. W.; Sandvik, E. I. Evaluation of

polymer flooding in a layered reservoir with crossflow, retention, and degradation. Society of Petroleum Engineers Journal, v. 16, n. 02, p. 82-96, 1976.

Wan, H.; Seright, R. S. Is Polymer Retention Different Under Anaerobic vs. Aerobic Conditions. SPE Journal, v. 22, n. 02, p. 431-437, 2017.

Willhite, G. P.; Dominguez, J. G. Mechanisms of polymer retention in porous media. Improved oil recovery by surfactant and polymer flooding. p. 511-554, 1977.

Zaitoun, A.; Kohler, N. The role of adsorption in polymer propagation through reservoir rocks. IN: SPE INTERNATIONAL SYMPOSIUM ON OILFIELD CHEMISTRY, 1987, San Antonio. Proceedings…San Antonio: Society of Petroleum Engineers, 1987.

Zhang, G.; Seright, R. Effect of concentration on HPAM retention in porous media. SPE Journal, v. 19, n. 03, p. 373-380, 2014.

Zhang, G.; Seright, R. S. Hydrodynamic Retention and Rheology of EOR Polymers in Porous Media. IN: SPE INTERNATIONAL SYMPOSIUM ON OILFIELD CHEMISTRY. 2015, The Woodlands. Proceedings…The Woodlands: Society of Petroleum Engineers, 2015.

Zheng, C. G.; Gall, B. L.; Gao, H. W.; Miller, A. E.; Bryant, R. S. Effects of polymer adsorption and flow behavior on two-phase flow in porous. SPE Reservoir Evaluation & Engineering, v. 3, n. 03, p. 216-223, 2000.

Simetric convertion factors				
cp	x1.0*	E-03	=	Pa.s
psi	x6.894 757	E+00	=	KPa
md	x9.869 233	E-01	=	μm^2
*Converstion factor is exact				

Reception: July 10, 2019
Acceptance: July 11, 2020